

Progressive development of quartz fabrics in a shear zone from Monte Mucrone, Sesia-Lanzo Zone, Italian Alps

H. VAN ROERMUND, G. S. LISTER and P. F. WILLIAMS

Department of Tectonics, Geological Institute, University of Leiden, Leiden, The Netherlands

(Received 26 September 1978; accepted in revised form 13 December 1978)

Abstract— Quartz *c*-axis fabrics are described from a shear zone in a jadeite – garnet bearing meta-granite from Monte Mucrone, in the Sesia-Lanzo Zone of the western Italian Alps. Quartz blebs in the meta-granitoid are progressively deformed into cigar shaped lenses, and are recrystallized. Fabrics measured from individual blebs show considerable variation resulting from an initial orientation effect, and are not very enlightening. A synoptic diagram, however, has a pole-free area which can be correlated with the extension direction, and an asymmetry which is consistent with the known sense of shear operating in the zone.

Although the technique of preparing synoptic diagrams is rather painstaking, its use is advocated for complex fabric situations, as it may allow partial removal of problems associated with non-random initial orientation distributions.

INTRODUCTION

IN SHEAR ZONES of the type described by Ramsay & Graham (1970) the bulk deformation path may have approximated to progressive simple shear. It is interesting to study such zones to see if crystallographic fabrics in quartz are controlled in orientation by the kinematic framework as predicted by the generalized Taylor–Bishop–Hill analysis (Lister 1977, Lister & Price 1978), or alternatively, are related directly to the finite strain axes as suggested by previous data (e.g. Hara *et al.* 1973, Carreras *et al.* 1977).

In the ideal case of a shear zone undergoing heterogeneous simple shear (Fig. 1a) the finite strain axes and the instantaneous stretching axes do not coincide in orientation. If preferred orientation is controlled by the state of finite strain, the pattern elements of developing crystallographic fabrics should rotate with increasing shear strain, tracking the trajectories of the axes of finite strain (Fig. 1b). If the kinematic framework is the controlling factor, fabrics will develop in relation to the orientation of the flow plane, and the instantaneous stretching axes. If the kinematic axes are constant in orientation the pattern elements will also remain constant in orientation throughout the shear zone (Fig. 1c) only varying in the strength of *c*-axis concentrations, for the ideal case.

The generalized Taylor–Bishop–Hill analysis predicts that the symmetry of a crystallographic fabric is equal to the symmetry common to the deformation path and the initial orientation distribution. In a number of cases asymmetry in quartz fabrics can be used to confirm sense of shear in shear zones (e.g. Bouchez 1977). However because the population of initial grain orientations also affects the symmetry of deformation fabrics, this result is not as useful as it at first appears. For example, Lister & Price (1978, fig. 17) show an initial fabric can cause asymmetry unrelated to the sense of movement, and Eisbacher (1970) documents effects that vary from one recrystallized quartz domain to another.

MICROSTRUCTURE

The investigated sample comes from a deformed, metamorphosed stock of granitic to quartz-dioritic composition from the Sesia-Lanzo Zone near Biella. This metagranitoid has suffered a complex metamorphic history including high-pressure low temperature metamorphism (Compagnoni & Maffeo 1973). The deformation responsible for the shear zones post-dates the main high-pressure event but has otherwise not been characterized.

Quartz in the meta-granitoid outside the shear zone occurs in blebs comprising one or several large grains. In approaching the centre of the shear zone these blebs become progressively more deformed and appear as prolate ellipsoid shaped lenses that are more and more parallel to the walls of the zone. The lenses are heterogeneously deformed (Fig. 2) but their aspect ratio gives a semi-quantitative measure of the amount of strain, and of the approximate location of the finite strain axes (Fig. 1a). The shear direction is assumed to be parallel to the walls of the zone, and orthogonal to the axis of curvature of the quartz blebs. From the geometry of the latter the sense of shear is also evident (Fig. 3).

The large quartz grains show evidence of increasing recrystallization with increasing strain. In the meta-granitoid near the shear zone, the large (up to 1 cm) old grains are surrounded by smaller recrystallised grains (less than 2 mm). The old grains have undulose extinction, with sub-grain boundaries parallel to prism planes, and many types of deformation lamellae. Commonly these lamellae intersect prism planes at 40–50° suggesting near rhomb or pyramidal orientations.

The less deformed recrystallized quartz domains exhibit little undulose extinction and display a well developed foam-microstructure (Fig. 4) suggesting that surface free energy played an important role in producing the final microstructure.

In most deformed parts of the quartz lenses, grain-boundary pinning can be observed (Fig. 5). This is inter-

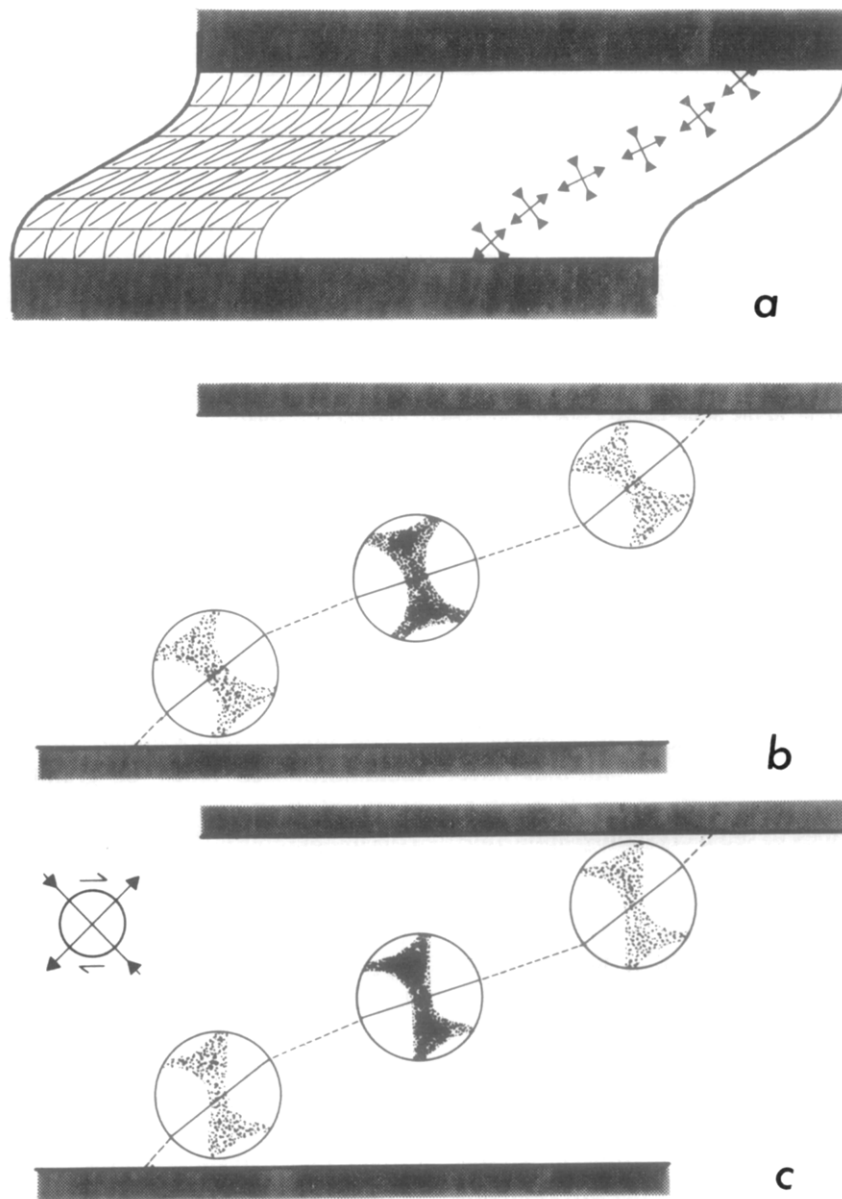


Fig. 1(a). Model of an ideal heterogeneous simple shear zone. The deformation at every point of the shear zone is progressive simple shear. The trajectories of the axes of finite strain are shown. The orientation of the instantaneous stretching axes remains constant at 45° to the shear plane throughout the zone. 1(b) A type I crossed girdle pattern (Hara *et al.* 1973) formed in a symmetric relationship to the axes of finite strain will rotate as shown. The trajectory of the finite axis of extension is indicated. 1(c) Extrapolations from the predictions of the Taylor-Bishop-Hill analysis suggest that a type I crossed girdle pattern will develop in progressive simple shear as shown. Note that an ideal shear zone is considered, where each grain undergoes progressive simple shear. The characteristics to note are: (i) there is a girdle of *c*-axes orthogonal to the shear direction; (ii) there is a distinct asymmetry; (iii) with increase in shear strain, maxima and girdles become more intense but do not change their orientation with respect to the shear plane, assumed to be parallel to the walls of the zone.

preted as indicating that elastic distortional energy within the quartz grains played an important role in driving high angle grain boundary migration.

The different microstructures do not have to be interpreted as spatial reflections of time sequences. An alternative interpretation is that the differences are related to variation in strain rate, as for example in the following scheme. In less deformed parts, strain rates were lower so that during recrystallization, surface energy microstructures were able to develop. In the high strain rate parts, it is suggested that recovery was not fast enough to prevent the build up of elastic energy associated with lattice distortion around individual dislocations and dislocation walls, to the extent where this elastic potential energy was sufficient to drive

migration of existing high angle grain boundaries. Such an interpretation of the pattern variation in quartz microstructures is consistent with the hypothesis that they formed as a result of a single deformation that produced the shear zone. However it is likely that microscopically and sub-microscopically visible structures have been influenced by the closing stages of deformation, during stress relaxation, and while strain rate decayed towards zero.

QUARTZ-FABRICS

Using an universal stage quartz fabrics have been measured from the undeformed rock through to the centre of the zone.

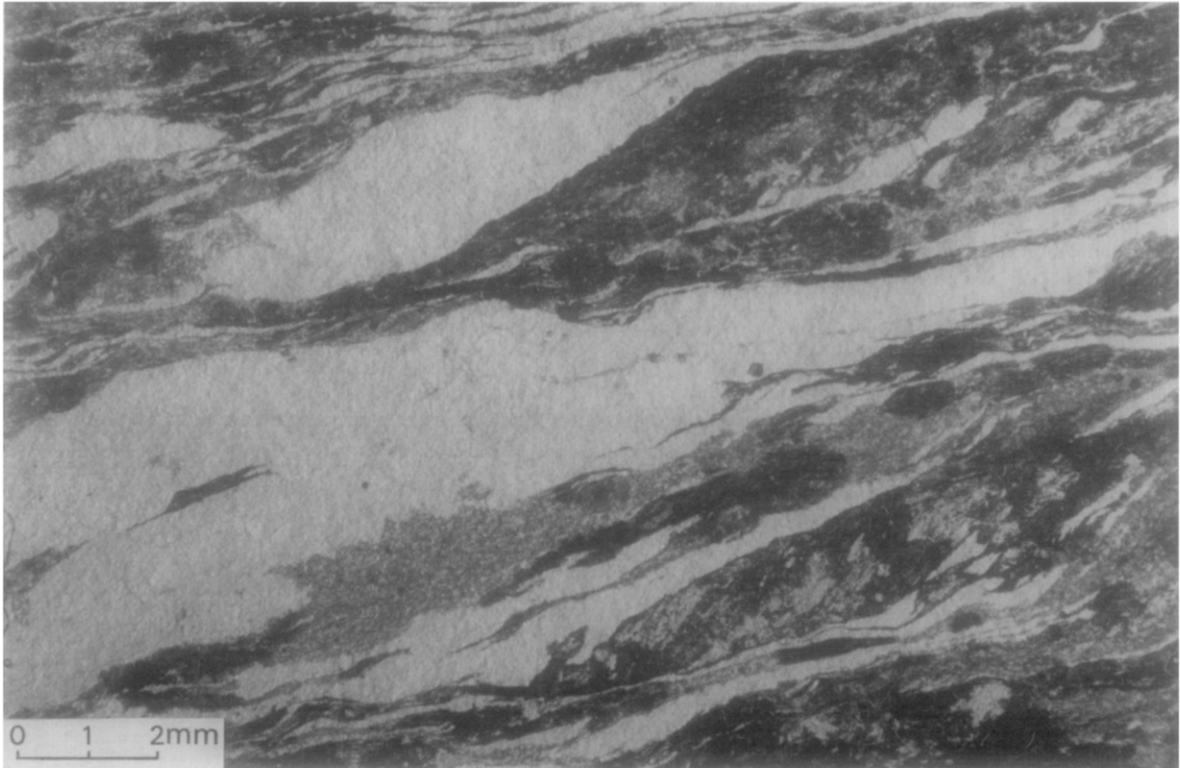


Fig. 2. Heterogeneously deformed quartz lenses in the shear zone. Section cut parallel to the lineation and normal to the wall. The microstructures within the different domains are discussed in the text. Plane polarised light.

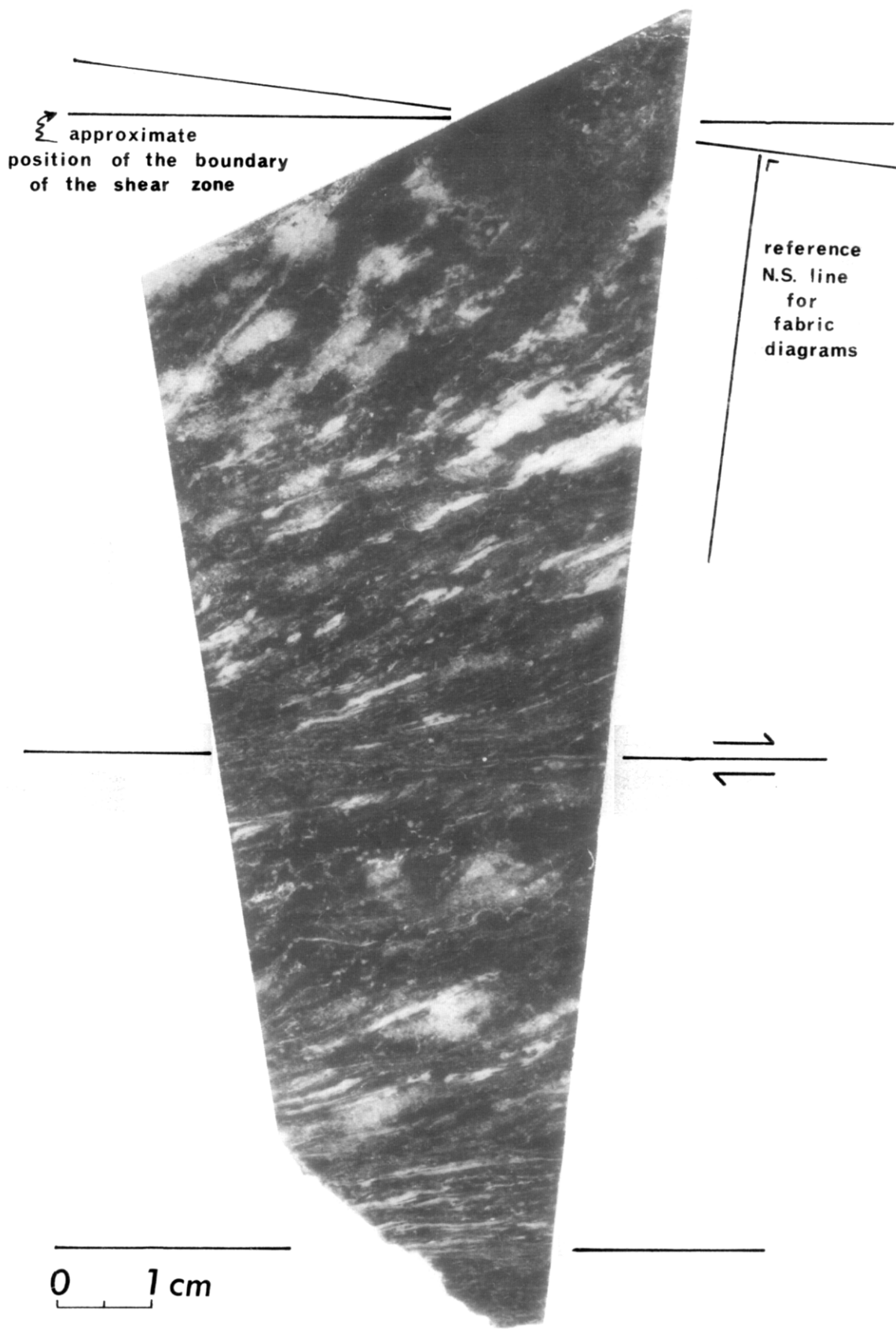


Fig. 3. The investigated, inhomogeneously deformed, shear zone. Indicated on the diagram are the sense of shear, the maximum attitude of the long axis of finite strain at different parts of the shear zone and the approximate position of the boundary of the shear zone. For coordination with fabric diagrams elsewhere in the text the used reference system is also indicated on the diagram.

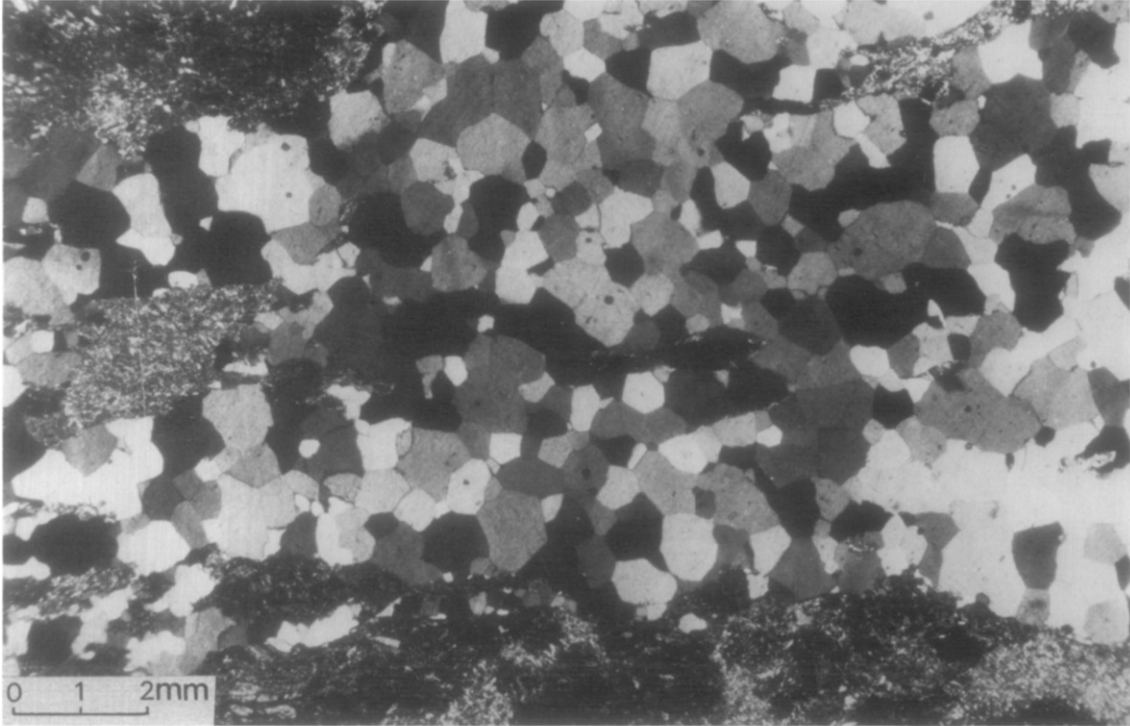


Fig. 4. Quartz foam texture in less deformed regions of quartz. Crossed nicols.

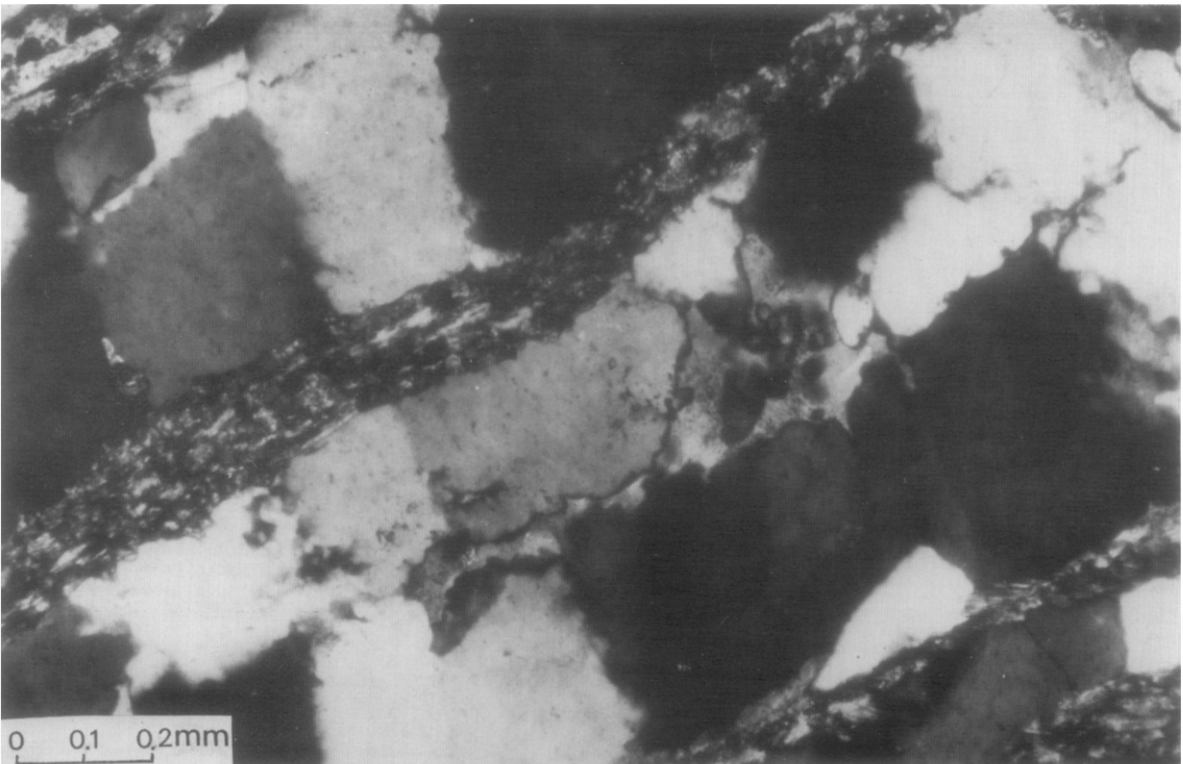


Fig. 5. Serrated, locally pinned quartz grain boundaries in the most deformed regions of quartz grains. Crossed nicols.

An attempt was made to discern orientation relationships between old grains in the quartz blebs and the new generation of grains. The histogram of old-grain, new-grain orientations (Fig. 6) suggests that there is a lack of relationships greater than 60° . Most controlled phenomena linked with grain growth effects are therefore to be expected. An attempt was also made to determine the orientation pattern of quartz grains in the meta-granitoid adjacent to the shear zone. This is not easy as only a few grains occur in each thin section. However, small, perhaps only slightly deformed, quartz blebs are often more completely recrystallized than the larger domains. Figure 7 shows *c*-axis fabrics in some of these recrystallized domains. The patterns are not reproducible and the empty-space test proposed by Chayes (1949) indicates a near random pattern. Thus, although recrystallization is related to the shear zone, it is concluded that no preferred orientation existed before the shear zone was produced.

Quartz *c*-axis fabrics in several different lenses were then measured. These patterns are depicted in Figs. 8(a-c) for the most deformed quartz domains. There is a fabric in each case but it is not clear what pattern the elements define. The patterns could be either intersecting great circle girdles, or small circle girdles about the approximate position of the axis of shortening, with a great circle girdle almost perpendicular to the interpreted shear direction. The patterns are not distinct enough to reach an unequivocal conclusion. Fabrics in less deformed quartz lenses are more scattered, although preferred orientations do exist (Fig. 9). In the

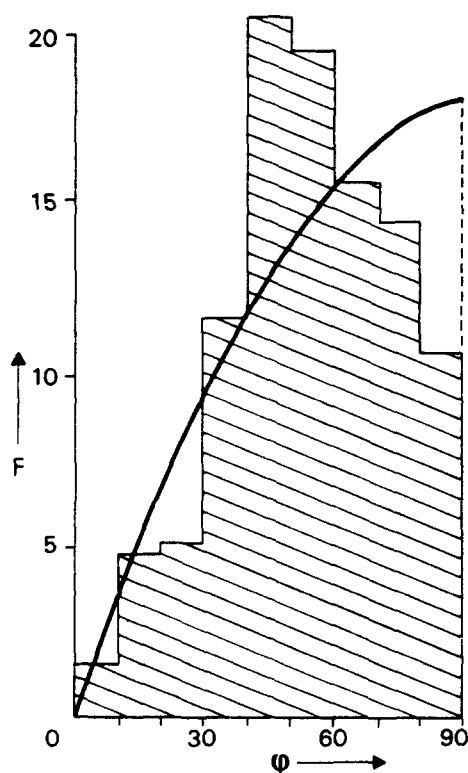


Fig. 6. Histogram showing the frequency (*F*) of angles ϕ between *c*-axes of new grains and the adjacent old grain. Superimposed on the histogram is a curve showing the theoretical distribution of angles between a fixed line and a continuous population of randomly oriented lines.

least deformed part of the shear zone a pattern was also obtained, and there is the suggestion of a girdle almost perpendicular to the interpreted shear direction (Fig. 10). However, again, the pattern is not well enough developed to rule out other possibilities.

DISCUSSION

Several different maxima orientations are found in the collection of fabric diagrams. The reason for this probably relates to the limited number of initial orientations given by the few old-grains which formed the original quartz blebs. During deformation in the shear zone it is supposed that the initial orientation distribution was spread and scattered, mainly as a result of recrystallization, but also because of subgrain formation. This scattering process was not sufficient however to obliterate the effect of a non-random starting population in the observed deformation fabrics, hence the variation in maximum orientation.

During the development of a deformation fabric we suggest that reorientation of crystal axes takes place along specific rotation paths, which may be traced on a pole figure or inverse pole figure (Lister in press). This means that the re-orientation trajectories together with the initial orientation distribution determine how a particular deformation fabric will develop. Effects of a variable initial orientation population will show up as a variation in maximum orientation and intensity distribution. This is because specific groups of initial orientations 'feed' different maxima in the final fabric.

By combining data from each fabric diagram one might be able to eliminate the effect of the starting population. In practice this is not generally possible because sufficient diversity in orientation exists to eliminate the chance of clear definition of an underlying fabric. However by constructing a synoptic plot of all maxima (in this case above 2.5% per 1% area) and pole free areas, some of this scatter is avoided.

In favourable circumstances the synoptic diagram will define the 'skeleton' or 'framework' of the deformation fabric that would have developed in any one volume of the rock, if that volume had initially contained a random orientation population.

The synoptic plot prepared from the preceding diagrams (Fig. 11) has the following characteristics: (a) a great circle girdle orthogonal to the direction of shear, this girdle becomes broader from the centre (20°) towards the periphery (50°); (b) a pole free area containing the interpreted kinematic and finite extension axes. The orientation of the kinematic and the finite extension axes are determined as is illustrated in Fig. 1(a); (c) a small pole free area about the interpreted kinematic shortening axis; and (d) it is asymmetric.

Despite the fact that data for the synoptic diagram were collected from blebs that have undergone various amounts of strain, and thus have differently orientated finite strain axes, the synoptic fabric is what we might expect from a single domain. This point is worth further examination.

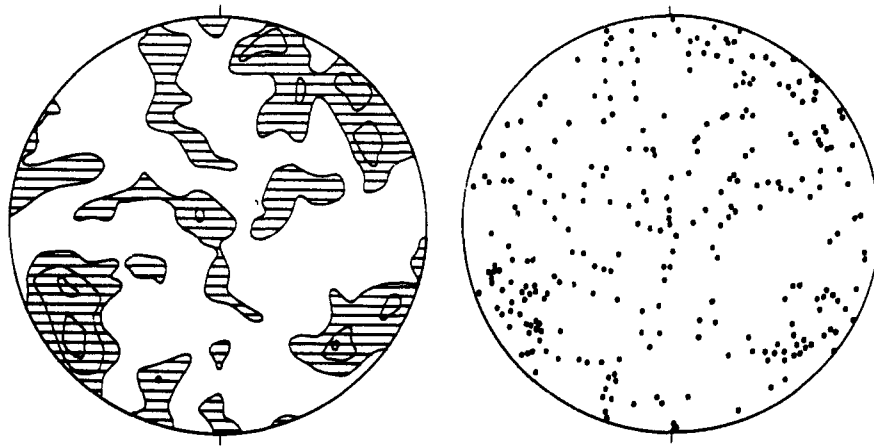


Fig. 7. Quartz *c*-axes fabric diagram from outside the shear zone 300 measurements. Lower hemisphere. Contours: 1, 2, 3% per 1% area.

The sub-fabrics do not give well defined patterns, for reasons discussed above, but certain features can be recognized in most diagrams, specifically the girdle and the pole free areas. If we examine the relationship between these pattern elements and the shear plane, we find a constant orientation despite demonstrable variation in the attitudes of the finite strain axes.

The Taylor-Bishop-Hill analysis (Lister *et al.* 1978) predicts that fabric should be related to kinematic axes

rather than finite strain axes, and specifically predicts girdles of *c*-axes normal to the shear plane, as illustrated in Fig. 1(c). It is difficult with data of the type presented here to be sure of significance. However, with this limitation in mind, if we assume progressive simple shear in each domain, the data support the hypothesis that quartz fabrics are controlled in orientation by the kinematic framework. The theory also predicts that the strength of the fabric is related to the amount of finite

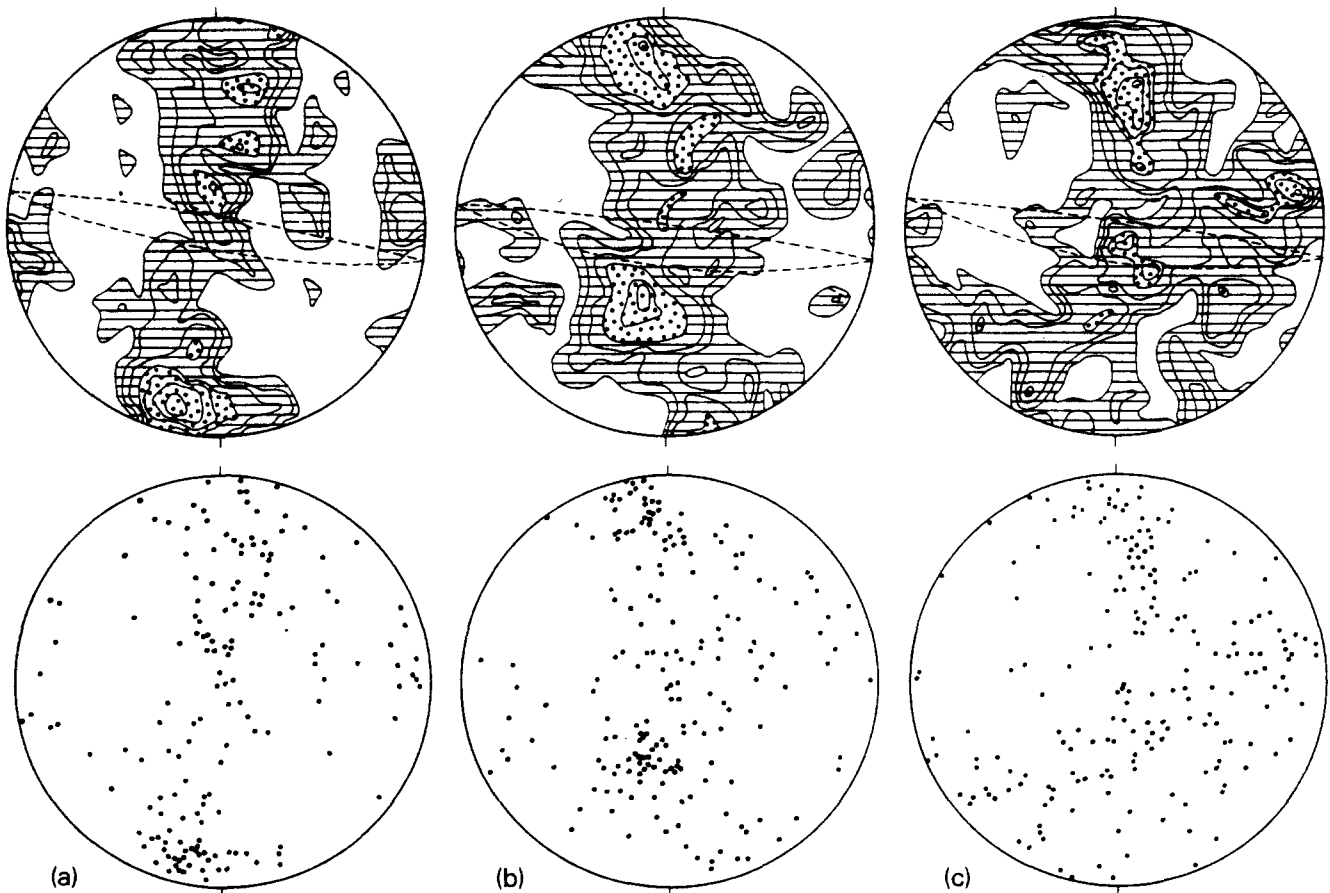


Fig. 8. Quartz *c*-axes fabric diagrams from the most deformed parts of the shear zone. 8(a) 156 measurements. 8(b & c) 200 measurements. Lower hemisphere. Contours—8(a) at 0.5, 1, 1.5, 2.5, 3.5, 5, 6%, 8(b) at 0.5, 1, 1.5, 2.5, 5, 7%, 8(c) at 0.5, 1, 1.5, 2.5, 3, 4.5%, all per 1% area.

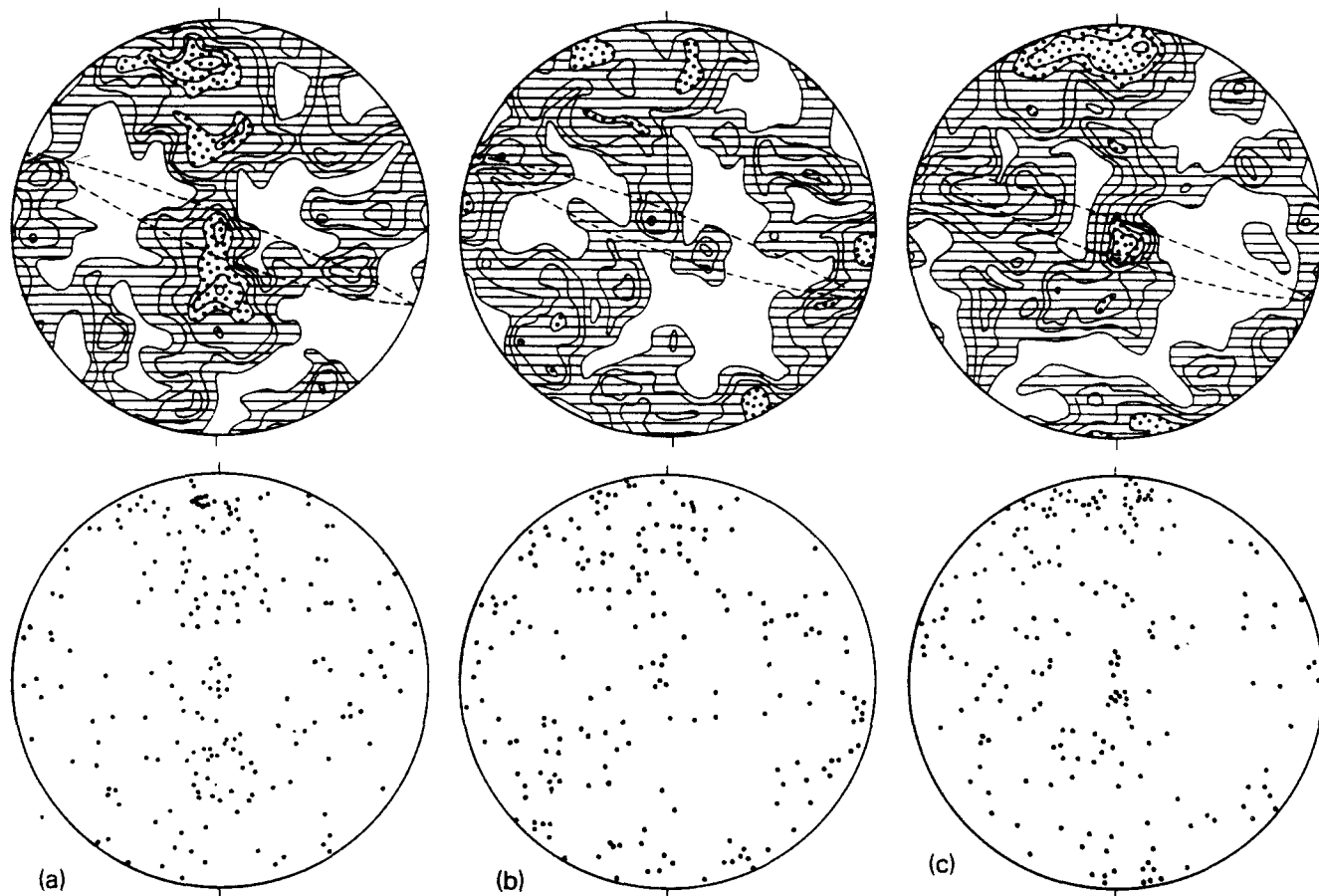


Fig. 9. Quartz *c*-axes fabric diagrams from less deformed parts of the shear zone. 9(a-c) 200 measurements. Lower hemisphere. Contours—9(a) at 0.5,1,1.5,2.5,3.5,5%, 9(b) at 0.5,1,1.5,2.5%, 9(c) at 1,1.5,2.5,5,6% all per 1% area.

strain, and this is also supported by the data in that the best defined fabrics come from the most deformed blebs.

Other workers (e.g. Carreras *et al.* 1977, Hara *et al.* 1973) have demonstrated a relationship between fabric orientation and the axes of finite strain, so we are apparently faced with a contradictory situation. This could perhaps be resolved by considering the role of discon-

tinuities during plastic deformation, but for the moment more data need to be collected concerning fabric development in shear zones.

Acknowledgements—The photographs in this paper were prepared by W. C. Laurijssen and H. Schiet, the diagrams by J. Bult, and the authors thank them for their valuable cooperation.

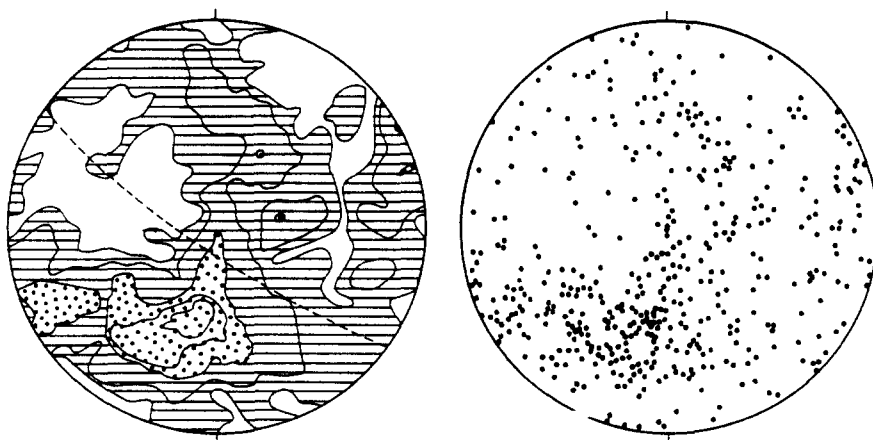


Fig. 10. Quartz *c*-axes fabric diagram from the periphery of the shear zone. 454 measurements. Lower hemisphere. Contours—0.5,1,2,3,4% per 1% area.

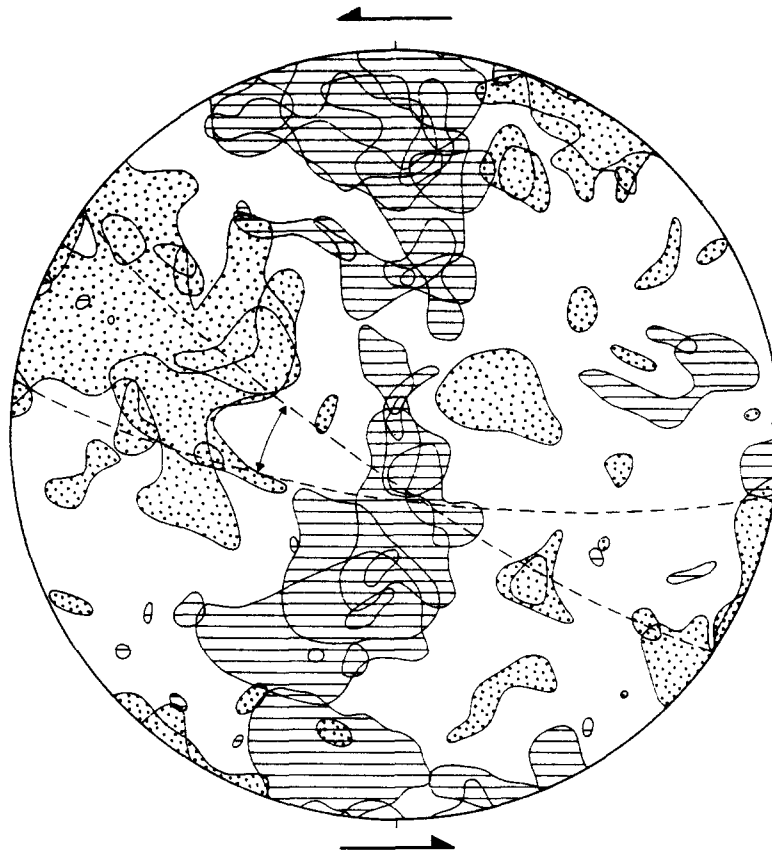


Fig. 11. Synoptic diagram showing: horizontally striped areas: maxima with concentrations greater than 2½% per 1% area from fabric diagrams from Figs. 8(a-c), 9(a-c) and 10. Black stippled areas: completely pole free areas of the fabric diagrams from Figs. 8(b&c), 9(a&b) and 10. The dashed lines on the diagram represent the total variation in attitude of the long axes of the deformed quartz blebs.

REFERENCES

- Bouchez, J. L. 1977. Plastic deformation of quartzites at low temperature in an area of natural strain gradient. *Tectonophysics* **39**, 25-50.
- Carreras, J., Estrada, A. & White, S. 1977. The effects of folding on the *c*-axis fabrics of a quartz mylonite. *Tectonophysics*, **39**, 3-24.
- Chayes, F. 1949. Statistical analysis of fabric diagrams. In: *Structural Petrology of Deformed Rocks*. (edited by Fairbairn, H. W.) Addison-Wesley, Cambridge, MA.
- Compagnoni, R. & Maffeo, B. 1973. Jadeite bearing metagranites i.s. and related rocks in the Mt. Mucrone area (Sesia-Lanzo Zone, Western Italian Alps). *Schweiz. miner. petrogr. Mitt.* **53**, 355-378.
- Eisbacher, G. H. 1970. Deformation mechanisms of mylonite rocks and fractured granites in Cobequid-Mountains, Nova Scotia, Canada. *Bull. geol. Soc. Am.* **81**, 2009-2020.
- Hara, I., Takeda, K. & Kimura, T. 1973. Preferred lattice orientation of quartz in shear deformation. *J. Sci. Hiroshima Univ. Ser. C7*, 1-11.
- Lister, G. S. 1977. Discussion: crossed-girdle *c*-axes fabrics in quartzites plastically deformed by plane strain and progressive simple shear. *Tectonophysics* **39**, 51-54.
- Lister, G. S. in press. Texture transitions in plastically deformed calcite rocks. *Proc. 5th Int. Conf. Textures of Metals.*, Aachen, Germany, February, 1978. To be published.
- Lister, G. S. & Price, G. P. 1978. Fabric development in a quartz-feldspar mylonite. *Tectonophysics* **49**, 37-78.
- Lister, G. S., Paterson, M. S. & Hobbs, B. E. 1978. The simulation of fabric development in plastic deformation and its application to quartzite: the model. *Tectonophysics* **45**, 107-158.
- Ramsay, J. G. & Graham, R. H. 1970. Strain variation in shear belts. *Can. J. Earth Sci.* **7**, 786-813.